

1 **Usefulness of the pancreas as a prime target for histopathological diagnosis of *Tilapia***
2 ***parvovirus* (TiPV) infection in Nile tilapia, *Oreochromis niloticus***

3 Ha Thanh Dong^{1*}, Pattiya Sangpo², Le Thanh Dien³, Thao Thu Mai⁴, Nguyen Vu Linh⁵, Jorge
4 del-Pozo⁶, Krishna R Salin¹, Saengchan Senapin^{2,7*}

5 ¹AARM/FAB, School of Environment, Resources and Development, Asian Institute of
6 Technology, Pathum Thani, Thailand

7 ²Fish Heath Platform, Center of Excellence for Shrimp Molecular Biology and Biotechnology
8 (Centex Shrimp), Faculty of Science, Mahidol University, Bangkok, Thailand

9 ³Faculty of Applied Technology, School of Engineering and Technology, Van Lang University,
10 Ho Chi Minh City, Vietnam

11 ⁴Division of Aquacultural Biotechnology, Biotechnology Center of Ho Chi Minh City, Ho Chi
12 Minh, Vietnam

13 ⁵Department of Animal and Aquatic Sciences, Faculty of Agriculture, Chiang Mai University,
14 Chiang Mai, 50200, Thailand

15 ⁶Easter Bush Pathology, Royal (Dick) School of Veterinary Studies, Edinburgh, UK

16 ⁷National Center for Genetic Engineering and Biotechnology (BIOTEC), National Science and
17 Technology Development Agency (NSTDA), Pathum Thani, Thailand

18

19 **Running title:** Histopathological landmark of TiPV

20 Corresponding authors:

21 H. T. Dong, E-mail: httdong@ait.ac.th

22 S. Senapin, E-mail: saengchan@biotec.or.th

23 **Abstract**

24 *Tilapia parvovirus* (TiPV) is an emerging virus reportedly associated with disease and mortality
25 in farmed tilapia. Although previous descriptions of histopathological changes are available, the
26 lesions reported in these are not pathognomonic. Here, we report Cowdry type A inclusion
27 bodies (CAIB) in the pancreas as a diagnostic histopathological feature found in adult Nile
28 tilapia naturally infected with TiPV. This type of inclusion body has been well-known as a
29 histopathological landmark for the diagnosis of other parvoviral infections in shrimp and
30 terrestrial species. Interestingly, this lesion could be exclusively observed in pancreatic acinar
31 cells, both in the hepatopancreas and pancreatic tissue along the intestine. *In situ* hybridization
32 (ISH) using a TiPV-specific probe revealed the intranuclear presence of TiPV DNA in multiple
33 tissues, including the liver, pancreas, kidney, spleen, gills, and the membrane of oocytes in the
34 ovary. These findings suggest that although TiPV can replicate in several tissue types, CAIB
35 manifest exclusively in pancreatic tissues. In addition to TiPV, most diseased fish were co-
36 infected with *Streptococcus agalactiae*, and presented with multifocal granulomas secondary to
37 this bacterial infection. Partial genome amplification of TiPV was successful and revealed high
38 nucleotide identity (> 99%) to previously reported isolates. In summary, this study highlights the
39 usefulness of pancreatic tissue as a prime target for histopathological diagnosis of TiPV in
40 diseased Nile tilapia. This pattern may be critical when determining the presence of TiPV
41 infection in new geographic areas, where ancillary testing may not be available. TiPV
42 pathogenesis in this landmark organ warrants further investigation.

43 **Keywords:** Cowdry type A, histopathology, tilapia, *tilapia parvovirus*, TiPV, pathognomonic
44 lesion

45 **Introduction**

46 Tilapia (*Oreochromis* spp.) is an aquatic animal species widely cultured in over 100 countries,
47 where global production is approximately 6.5 million tons per year (FAO, 2020). The
48 intensification of tilapia farming industry has been confronted with an increasing number of
49 emerging infectious diseases (Ferguson et al., 2014; Eyngor et al., 2014; Machimbirike et al.,
50 2019; Dong et al., 2019; Ramírez-Paredes et al., 2020). For instance, in the past five years,
51 widespread occurrence of disease outbreaks caused by two emerging viruses, namely tilapia lake
52 virus (TiLV) and infectious spleen and kidney necrosis virus (ISKNV), has highlighted the
53 critical need for rapid, accurate diagnostics to aid in the control or mitigation of emerging
54 diseases (Machimbirike et al., 2019; Ramírez-Paredes et al., 2020).

55 A novel parvovirus, termed *Tilapia parvovirus* (TiPV), was initially discovered from the fecal
56 samples of tilapia-fed crocodiles and intestine samples of tilapia from Hainan, China using next-
57 generation sequencing (Du et al., 2019). However, there was no evidence that this virus was
58 associated with disease in tilapia at that point. Then, Liu et al. (2020) reported their findings of
59 an outbreak investigation involving severe mortality (approx. 60-70%) of adult tilapia (500-600
60 g) in Hubei, China, since 2015. The diseased fish displayed signs of lethargy, anorexia, abnormal
61 swimming behavior (e.g., corkscrew movements), cutaneous hemorrhages, exophthalmia, and
62 severe ocular lesions on rare occasions (Liu et al., 2020). In this case, although coinfection of
63 TiPV and *Streptococcus agalactiae* was detected in clinically sick fish, TiPV was isolated,
64 propagated in tilapia brain cells (TiB), characterized, and was proved to be pathogenic on its own
65 through experimental infection (reaching ~90% mortalities at 11 dpi).

66 TiPV is a non-enveloped, spherical virus with a diameter of 30 nm. The TiPV genome contains
67 4,269 bp linear single-stranded DNA (ssDNA), including 208 bp 5' UTR, 396 bp ORF1, 1875 bp
68 non-structural protein 1 (NS1), 504 bp NS2, 216 bp ORF2, 1665 bp capsid protein 1 (VP1), and
69 46 bp 3' UTR (Liu et al., 2020). TiPV is currently considered a novel *Chapparvovirus* of the
70 *Parvoviridae* family (Du et al., 2019; Liu et al., 2020).

71 Recently, cases of TiPV infection in hybrid red tilapia were reported in Thailand. The majority
72 of fatalities occurred as a result of complicated coinfection between tilapia lake virus (TiLV) and
73 TiPV, mainly in juveniles (10-30 g), with recorded cumulative mortality rates of 50-75%.

74 Lethargy, hemorrhage, cutaneous ulceration, exophthalmos, and abnormal swimming were all
75 observed in diseased fish (Yamkasem et al., 2021; Piewbang et al., 2022).

76 To date, pathognomonic lesions serving as the histopathological landmark for diagnosis of TiPV
77 have not been reported. Non-specific histopathological changes reported previously included
78 tissue degeneration/necrosis, inflammatory infiltration by lymphocytes and macrophages,
79 increased numbers of melano-macrophage centers, etc. (Du et al., 2019; Liu et al., 2020;
80 Yamkasem et al., 2021; Piewbang et al., 2022). Here, we report the presence of characteristic
81 Cowdry type A inclusion bodies (CAIB) in the pancreatic tissues during TiPV infection, which
82 may be pathognomonic, and suggest the usefulness of the pancreas as a prime target for
83 histopathological diagnosis of TiPV diseased tilapia. More insights into tissue tropism and
84 localization of TiPV in various infected tissues have also been unveiled.

85 **Materials and Methods**

86 **Fish samples and preservation**

87 In 2020, we received a set of 10 naturally diseased adult Nile tilapia from an affected breeding
88 farm for disease diagnostics. According to the farm owner, less than 1% of fish in the population
89 showed signs of sickness and only minor mortalities were recorded after handling stress. Freshly
90 dead fish (n=9) were subjected to bacterial isolation, using Tryptic Soy Agar (TSA, Becton,
91 Dickinson, USA) as general medium and *Streptococcus agalactiae* Selective Agar (SSA,
92 HiMedia, India) as a selective medium for *S. agalactiae*. Internal organs (i.e., liver, kidney,
93 spleen, gills, and intestine) from 9 fish were preserved in 10% neutral buffered formalin for
94 histological examination and *in situ* hybridization analysis. The spleen and liver tissues were also
95 preserved in 95% ethanol for molecular diagnostics.

96 **Histological analysis**

97 Tissue samples were preserved overnight in a 10% neutral buffer formalin solution before being
98 transferred to 70% ethanol for histology. Tissue processing involved dehydration, paraffin
99 embedding, sectioning at 5 μ m thickness, and staining with hematoxylin and eosin (H&E). Light
100 microscopy with a digital camera was used to examine histopathological changes.

101 **Quantitative polymerase chain reaction (qPCR) detection of TiPV and *S. agalactiae***

102 The preserved spleen and liver samples were subjected to DNA extraction using the TF lysis
103 buffer method (Meemetta et al., 2020). DNA quantity and quality was measured using a
104 NanoDrop (Thermo Scientific, USA), with absorbance set at OD₂₆₀ and OD₂₈₀. DNA samples
105 were diluted to 100 ng/µL for quantitative PCR (qPCR) reactions. Detection of TiPV was
106 performed using a protocol described by Liu et al. (2020). PCR mixtures were comprised of 10
107 µL 2X SYBR Green Master Mix (Bio-Rad, USA), 0.5 µL of each forward and reverse primers
108 (10 µM of each TiPV-Fq/TiPV-Rq) (Table 1), 2 µL DNA template and 7 µL ddH₂O. PCR was
109 performed at 94 °C for 2 min followed by 40 cycles of 94 °C for 10 s and 60 °C for 30 s. The
110 melting curve was analyzed in the last cycle. On the other hand, probe-based qPCR targeting
111 *groEL* gene was used to diagnose *S. agalactiae* infection, according to Leigh et al. (2019). The
112 qPCR reagents mixture contained 10 µL of 2X iTaq Universal Probes Supermix (Bio-Rad,
113 USA), 0.5 µL of 10 µM SagroEL-probe (Table 1), 1.8 µL of each primer SagroEL-F/R (10 µM),
114 3 µL of DNA template and 2.9 µL ddH₂O. The qPCR reaction was performed at 95 °C for 2 min
115 followed by 40 cycles of 95 °C for 5 s and 60 °C for 30 s. DNA extracted from *S. agalactiae*
116 2809 (Linh et al., 2021) was used as a positive control, and ddH₂O without DNA template was
117 used as a negative control.

118 **Amplification and sequence analysis of *NS1* and *VP1* genes of TiPV**

119 For confirmation of TiPV, full-length *NS1* (1857 bp) and *VP1* (1665 bp) were amplified using
120 newly designed primers, TiPV-NS1F/R and TiPV-VP1F/R (Table 1), respectively. The primers
121 were designed based on the complete genome sequence of TiPV (accession number MT393593).
122 Reaction mixtures comprised of 2 µL 10X PCR buffer, 0.4 µL of 10 mM dNTP, 0.4 µL of 50
123 mM MgCl₂, 0.5 µL of each forward and reverse primers (10 µM), 0.1 µL Taq polymerase
124 (Invitrogen, 5U/µL), 2 µL DNA template, and 14.1 µL ddH₂O. The PCR protocol started with a
125 pre-denaturation at 95 °C for 5 min followed by 30 cycles of denaturation at 95 °C for 30 s,
126 annealing at 60°C (for *NS1*) or at 54 °C (for *VP1*) for 30 s, extension at 72 °C for 2 min, and a
127 final extension at 72 °C for 5 min. PCR products were visualized on 1% agarose gel, and
128 expected amplicons of *NS1* and *VP1* genes were purified using Nucleospin® Gel and PCR clean-
129 up kit (Takara Bio, Japan). Purified PCR amplicons were individually subjected to Barcode-
130 Tagged sequencing (Celemics, Inc., South Korea). The obtained DNA sequences were processed
131 by Geneious Prime software (Biomatters, New Zealand) and analyzed using BLASTn from
132 NCBI database.

133 ***In situ* hybridization (ISH)**

134 Localization of TiPV in the infected tissues was investigated using an ISH assay. TiPV-specific
135 digoxigenin (DIG) labeling probe (359 bp) was synthesized using primers TiPV-Fq and TiPV-
136 NS1-R (Table 1) and DIG-labeling mix reagent (Roche, Germany) according to the
137 manufacturer's instructions. The PCR protocol included 30 cycles: pre-denature 94 °C for 5 min,
138 denature 94 °C for 30 s, annealing 55 °C for 30 s, extension 72 °C for 30 s, final extension 72 °C
139 for 2 min. The DNA-labeling probe was gel purified using Nucleospin® Gel and PCR clean-up
140 kit. An unrelated probe derived from a 282 bp fragment of shrimp infectious myonecrosis virus
141 (IMNV) (Senapin et al., 2007) was used as a negative control. The standard ISH procedure was
142 conducted with a probe concentration of 500 ng/slide (Dinh-Hung et al., 2021). Three
143 consecutive sections from each sample were assayed using a TiPV-specific probe, unrelated
144 probe, and H&E stain. The results were interpreted in parallel under a light microscope
145 connected to a digital camera.

146 **Results**

147 **Gross signs and histopathology**

148 Grossly, the fish submitted to our laboratory presented with loss of body condition, skin
149 erosions, cloudy eye lenses, and corneal injury (Figure 1A, B). Internal organs exhibited no
150 obvious abnormal changes in most individuals, except for rare instances of microhepatica,
151 intestinal pallor, and necrotic areas in the ovary (Figure 1C).

152 Histopathologically, Cowdry type A inclusion bodies (CAIB) in pancreatic acinar cells (in both
153 pancreatic islands of the hepatopancreas and pancreatic tissue along the intestine) were recorded
154 in all fish (Table 2). CAIB are intranuclear inclusions distinguished by chromatin margination
155 and a distinct, clear halo surrounding a central basophilic inclusion body (Figure 2A-D). There
156 were differences between CAIB size, ranging from small inclusions (early stage) similar to
157 nucleoli to eccentric, large inclusions with a well-defined halo (late stage) (Figure 2E).

158 Additionally, characteristic granulomas associated with intralesional bacterial cocci were
159 observed in the majority of the fish examined, most notably in the spleen, kidney, brain, and
160 ovary (Figure 3A-D). Typically, granulomas were filled with dark-brown pigment (consistent
161 with melanin). Numerous cocci bacteria (morphologically consistent with *Streptococcus* sp.)

162 were observed at high magnification in the necrotic core of some granulomas (Figure 3E) or
163 intracellularly on the membrane of oocytes (Figure 3F).

164 **Diseased fish tested positive for both TiPV and *S. agalactiae***

165 All examined fish ($n = 9$) were tested positive for TiPV by qPCR with Cq values ranging from
166 18.62 to 29.87 (Table 2). Subsequently, *NS1* and *VP1* of TiPV were successfully amplified from
167 representative samples and sequenced. Their partial ORF sequences of 1803 and 1414 bp were
168 submitted to GenBank under accession numbers OM884999 and OM885000, respectively. Blast
169 searches revealed that the *NS1* and *VP1* in this study have 99.5 and 99.22% nucleotide identities
170 to the *NS1* and *VP1* of the reference China TiPV strain TiPVC20160912 (accession no.
171 MT393593.1), respectively. Compared to the Thai TiPV strain KU01-TH/2020, the percent
172 nucleotide identity was 99.72% for the *NS1* (accession no. MW685502.1) and 99.58% for the
173 *VP1* (accession no. MW685502.1), respectively.

174 Six out of nine samples tested positive for *S. agalactiae* using *S. agalactiae* specific qPCR with
175 Cq ranging from 33.61 to 37.10. Pinpoint colony-forming bacteria were successfully cultured
176 from 3/9 fish, and all tested positive for *S. agalactiae* by qPCR (Table 1).

177 **Localization of TiPV in the infected tissue by ISH**

178 Using a DIG-labeled probe targeting a 359-bp fragment of the *NS1* gene of TiPV, there were
179 positive signals in multiple organs of TiPV infected fish, including the liver and pancreas (Figure
180 4) as well as the kidney, spleen, gills, and ovary (Figure 5). In contrast, no positive signal was
181 found when the same samples were assayed with an unrelated probe (negative control - Figure 4-
182 5). At the cellular level, TiPV positive signals were clearly localized to the nuclei and were noted
183 in hepatocytes (Figure 4A-C), pancreatic acinar cells (Figure 4D-F), renal tubular epithelial cells
184 (Figure 5A-C), splenic ellipsoids (Figure 5D-F), and cells within primary and secondary gill
185 lamella (Figure 5G-I). Notably, positive signals were also detected in cells around the oocyte cell
186 membrane in the ovary (Figure 5 J-L). CAIB were devoid of ISH signal (data not shown).

187 **Discussion**

188 This study reported the presence of CAIB in the pancreas of TiPV-infected tilapia for the first
189 time. This pathological feature was previously identified to be a histopathological landmark for
190 the diagnosis of two parvovirus infections in shrimp, namely hepatopancreatic parvovirus (HPV)

191 (recently called decapod hepanhamaparvovirus, DHPV) and infectious hypodermal and
192 haematopoietic necrosis virus (IHHNV) (Flegel et al., 2006; Srisala et al., 2021) and terrestrial
193 species (e.g. cattle, dogs, cats) (Kennedy & Palmer, 2016). Interestingly, the CAIB observed in
194 this study are similar to HPV inclusion bodies in shrimp, but the CAIB associated with TiPV
195 infection appear to be less numerous and smaller, requiring observation under high magnification
196 (100X). Although general histopathological changes have been reported, this previously
197 overlooked inclusion body is particularly useful for diagnosing TiPV due to its characteristic
198 morphology. Furthermore, CAIB were detected in the pancreas but not in other infected tissues,
199 demonstrating the pancreas' utility as a primary target for histopathological diagnosis of TiPV
200 infection in tilapia. This finding is important for identifying TiPV in new geographic locations,
201 which typically requires a combination of macroscopic, microscopic, and molecular
202 investigation. Also, this unique histopathological characteristic enables retrospective
203 investigation of TiPV infection in archived samples. It is possible to hypothesize that the
204 pancreas may present unique features in the pathogenesis and host-pathogen interaction of TiPV
205 infection in tilapia.

206 Although ISH with a TiPV-specific probe detected viral genomes in the nuclei of the cells from
207 multiple organs in TiPV infected tilapia, no hybridization signal was detected within CAIB. It is
208 possible that this is due to a defective replication cycle leading to aberrant accumulation of
209 virions lacking nucleic acid, or that the thickness of viral protein that makes up the inclusion
210 bodies prevents TiPV probe penetration. Interestingly, this phenomenon has also been observed
211 in shrimp parvovirus (per. comm., Prof. Tim W. Flegel), and warrants further investigation.
212 Similar to the previous reports (Liu et al., 2020; Piewbang et al., 2022), TiPV was detected in
213 various organs and cell types, indicating widespread cellular tropism, and the capability of
214 infecting tilapia systemically. This finding is interesting, as parvoviruses are reported to be
215 radiomimetic, i.e. they have tropism for dividing cells in other species (Boes and Durham, 2017),
216 a feature that would be expected to also occur in TiPV, and may suggest that division is ongoing
217 in adult tilapia in all of the tissues targeted by TiPV. Notably, the presence of TiPV positive
218 signals in oocyte membranes may indicate that this virus is capable of vertical transmission
219 similar to that of TiLV (Dong et al., 2020). However, more research would be necessary to
220 evaluate TiPV vertical transmission.

221 Although ISH was not done for *S. agalactiae* detection, the presence of dense intracellular cocci
222 bacteria was also occasionally observed in the epithelial membrane of oocytes in the degenerated
223 ovary of the affected female fish, providing supporting evidence for vertical transmission of this
224 agent (Pradeep et al., 2016).

225 The high nucleotide sequence similarity between the TiPV isolates in this study and those
226 reported previously in China and Thailand (Du et al., 2019; Liu et al., 2020; Yamkasem et al.,
227 2021) suggests that they may be from the same clone or have a highly conserved genomic nature.
228 Further genomic investigations could provide insight into viral epidemiology and evolution.

229 The disease event in this study could be attributed to TiPV and *S. agalactiae* coinfection. Similar
230 to a previous report, TiPV and *S. agalactiae* coinfection was associated with a disease outbreak
231 in adult tilapia in China. TiPV was also found in a relatively high prevalence (23.1 to 64.6 %) of
232 randomly collected samples without clinical signs in multiple geographical locations in China
233 (Liu et al. 2020). Most recently, TiPV and TiLV coinfections were found in the majority of
234 disease cases in juvenile tilapia in Thailand (Yamkasem et al., 2021; Piewbang et al., 2022).
235 Despite the fact that the fish population in this study was infected with both TiPV and *S.*
236 *agalactiae*, only a small proportion of mortality was observed after handling stress, implying that
237 both pathogens were in the chronic phase of infection. With respect to *S. agalactiae*, the presence
238 of numerous granulomas is marked as a histopathological feature of chronic infection. Taken
239 together, the available evidence indicates that additional research into the pathogenicity of TiPV
240 and risk factors for disease outbreaks is necessary to determine whether TiPV is a true pathogen
241 or an opportunistic agent. As TiPV has been described recently, its pathogenesis is unclear.
242 However, in view of this coinfection, it is possible to hypothesize that its presence may lead to
243 immunosuppression and facilitate secondary infection. For example, such an effect has been
244 reported in canine parvovirus type 2, feline panleukopenia virus, and bovine viral diarrhea
245 virus. In these instances, immunosuppression is interpreted as a direct result of lymphocytolysis
246 leading to lymphoid atrophy (Boes and Durham, 2017).

247 In conclusion, the present study described the presence of CAIB in the pancreas as a
248 histopathological landmark for the diagnosis of TiPV in tilapia. This pathological lesion is
249 unique to the pancreas, highlighting the critical nature of this tissue as a prime target for
250 histopathological diagnosis. Initial detection of CAIB is particularly helpful to suggest the need

251 for PCR, sequencing, and ISH analysis to identify TiPV infection. This is especially relevant for
252 TiPV diagnosis in countries or regions where it is reported for the first time, in order to facilitate
253 rapid diagnosis and emergent response to mitigate TiPV's negative impact on tilapia aquaculture.

254 **Acknowledgements**

255 This study was supported by BIOTEC Fellow's Research Grants (P-19-50170). H.T. Dong
256 acknowledges the Research Initiation Grant from the Asian Institute of Technology.

257 **Declaration of Competing Interest**

258 The authors declare that they have no known competing financial interests or personal
259 relationships that could have appeared to influence the work reported in this paper.

260 **Credit authorship contribution statement**

261 H.T.D., P.S., and S.S., conceptualization, methodology, investigation, writing original draft;
262 L.T.D., T.T.M., N.V.L., investigation, J.D.P., K.R.S., review-editing. All authors have read and
263 agreed to the current version of the manuscript.

264

265 **References**

266 Dinh-Hung, N., Sangpo, P., Kruangkum, T., Kayansamruaj, P., Rung-ruangkijkrai, T., Senapin,
267 S., Rodkhum, C., & Dong, H. T. (2021). Dissecting the localization of *Tilapia tilapinevirus* in
268 the brain of the experimentally infected Nile tilapia, *Oreochromis niloticus* (L.). *Journal of Fish
269 Diseases*, 44(8). <https://doi.org/10.1111/jfd.13367>

270 Dong, H. T., Senapin, S., Gangnonngiw, W., Nguyen, V. V., Rodkhum, C., Debnath, P. P.,
271 Delamare-Deboutteville, J., & Mohan, C. V. (2020). Experimental infection reveals transmission
272 of tilapia lake virus (TiLV) from tilapia broodstock to their reproductive organs and fertilized
273 eggs. *Aquaculture*, 515. <https://doi.org/10.1016/j.aquaculture.2019.734541>

274 Dong, H. T., Senapin, S., Jeamkunakorn, C., Nguyen, V. v., Nguyen, N. T., Rodkhum, C.,
275 Khunrae, P., & Rattanarojpong, T. (2019). Natural occurrence of edwardsiellosis caused by
276 *Edwardsiella ictaluri* in farmed hybrid red tilapia (*Oreochromis* sp.) in Southeast Asia.
277 *Aquaculture*, 499. <https://doi.org/10.1016/j.aquaculture.2018.09.007>

278 Du, J., Wang, W., Chan, J. F. W., Wang, G., Huang, Y., Yi, Y., Zhu, Z., Peng, R., Hu, X., Wu,
279 Y., Zeng, J., Zheng, J., Cui, X., Niu, L., Zhao, W., Lu, G., Yuen, K. Y., & Yin, F. (2019).
280 Identification of a Novel Ichthyic Parvovirus in Marine Species in Hainan Island, China.
281 *Frontiers in Microbiology*, 10. <https://doi.org/10.3389/fmicb.2019.02815>

282 FAO. *The State of World Fisheries and Aquaculture 2020. Sustainability in action.* FAO;
283 2020:244. <https://doi.org/10.4060/ca9229en>

284 Ferguson, H. W., Kabuusu, R., Beltran, S., Reyes, E., Lince, J. A., & del Pozo, J. (2014).
285 Syncytial hepatitis of farmed tilapia, *Oreochromis niloticus* (L.): A case report. *Journal of Fish*
286 *Diseases*, 37(6). <https://doi.org/10.1111/jfd.12142>

287 Flegel, T. W. (2006). Detection of major penaeid shrimp viruses in Asia, a historical perspective
288 with emphasis on Thailand. In *Aquaculture* (Vol. 258, Issues 1–4).
289 <https://doi.org/10.1016/j.aquaculture.2006.05.013>

290 Jubb, Kennedy & Palmer. Pathology of domestic animals. Volume II, pp 153-158. Ed: Maxie
291 M.G./ 2016 Elsevier.

292 Katie M. Boes, Amy C. Durham, in Pathologic Basis of Veterinary Disease (Sixth Edition),
293 2017, chapter 7, Elsevier.

294 Leigh, W. J., Zadoks, R. N., Costa, J. Z., Jaglarz, A., & Thompson, K. D. (2019). Development
295 and evaluation of a quantitative polymerase chain reaction for aquatic *Streptococcus agalactiae*
296 based on the *groEL* gene. *Journal of Applied Microbiology*. doi:10.1111/jam.14556

297 Liu, W., Zhang, Y., Ma, J., Jiang, N., Fan, Y., Zhou, Y., Cain, K., Yi, M., Jia, K., Wen, H., Liu,
298 W., Guan, W., & Zeng, L. (2020). Determination of a novel parvovirus pathogen associated with
299 massive mortality in adult tilapia. *PLoS Pathogens*, 16(9).
300 <https://doi.org/10.1371/journal.ppat.1008765>

301 Machimbirike, V.I., Jansen, M.D., Senapin, S., Khunrae, P., Rattanarojpong, T., Dong, H.T.
302 (2019). Viral infections in tilapines: More than just tilapia lake virus. *Aquaculture*, 503: 508-518.

303 Pradeep, P. J., Suebsing, R., Sirthammajak, S., Kampeera, J., Jitrakorn, S., Saksmerprome, V.,
304 Turner, W., Palang, I., Vanichviriyakit, R., Senapin, S., Jeffs, A., Kiatpathomchai, W., &
305 Withyachumanarnkul, B. (2016). Evidence of vertical transmission and tissue tropism of
306 Streptococcosis from naturally infected red tilapia (*Oreochromis* spp.). *Aquaculture Reports*, 3,
307 58–66. <https://doi.org/10.1016/J.AQREP.2015.12.002>

308 Ramírez-Paredes, J. G., Paley, R. K., Hunt, W., Feist, S. W., Stone, D. M., Field, T. R., Haydon,
309 D. J., Ziddah, P. A., Nkansa, M., Guilder, J., Gray, J., Duodu, S., Pecku, E. K., Awuni, J. A.,

310 Wallis, T. S., Verner-Jeffreys, D. W., & Biologicals Limited Ceva Santé, R. (2020). First
311 detection of infectious spleen and kidney necrosis virus (ISKNV) associated with massive
312 mortalities in farmed tilapia in Africa. <https://doi.org/10.1111/tbed.13825>

313 Senapin, S., Dong, H.T., Meemetta, W., Siriphongphaew, A., Charoensapsri, W.,
314 Santimanawong, W., Turner, W.A., Rodkhum, C., Withyachumnarnkul, B., Vanichviriyakit, R.
315 (2016). *Hahella chejuensis* is the etiological agent of a novel red egg disease in tilapia
316 (*Oreochromis* spp.) hatcheries in Thailand, *Aquaculture* 454, 1–7.

317 Senapin, S., Phewsaiya, K., Briggs, M., Flegel, T.W., 2007. Outbreaks of infectious myonecrosis
318 virus (IMNV) in Indonesia confirmed by genome sequencing and use of an alternative RT-PCR
319 detection method. *Aquaculture* 266, 32–38.

320 Yamkasem, J., Tattiyapong, P., & Surachetpong, W. (2021). Development and application of
321 TaqMan probe-based quantitative PCR assays for the detection of tilapia parvovirus. *Journal of*
322 *Fish Diseases*. <https://doi.org/10.1111/jfd.13565>

323 Yamkasem, J., Tattiyapong, P., Gorgoglione, B., & Surachetpong, W. (2021). Uncovering the
324 first occurrence of Tilapia parvovirus in Thailand in tilapia during co-infection with Tilapia
325 tilapinevirus. *Transboundary and Emerging Diseases*, 68(6). <https://doi.org/10.1111/tbed.14143>

326 **Tables and Figures**

327 **Table 1:** Primers used in this study

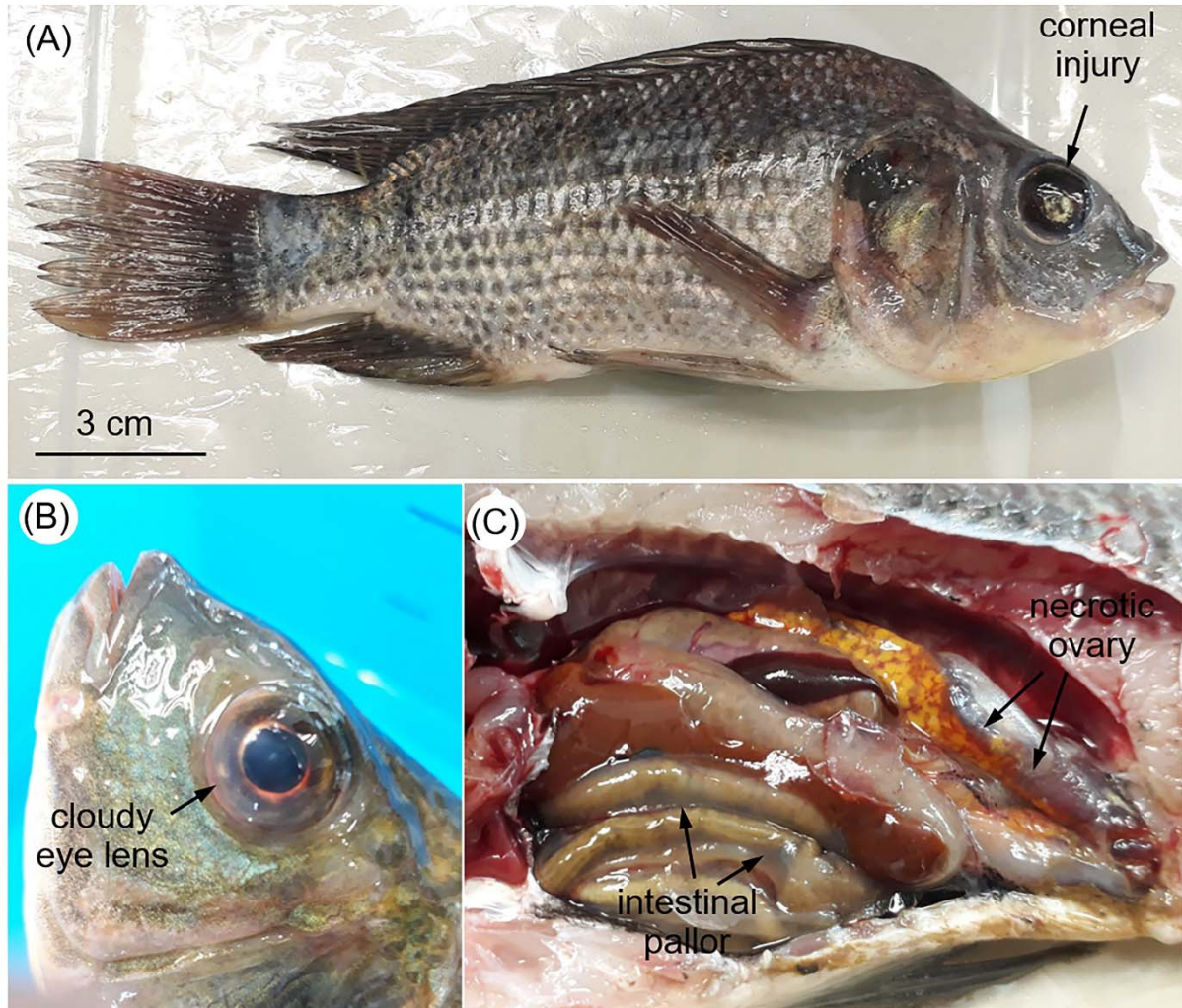
Primer name	Nucleotide sequence (5'-3')	Amplicon size (bp)	Target gene & pathogen	Usage	Reference
TiPV-Fq	GCACCAACAGCTGAGTACAAC	134	<i>NS1</i> , TiPV	qPCR detection	Liu et al., 2020
TiPV-Rq	AACTGCTCGGCTATCTCCTC				
TiPV-NS1-F	ATGCCTGTCTTCAGACTCGGAA	1857	<i>NS1</i> , TiPV	Gene amplification	This study
TiPV-NS1-R	TTAGCTCCGGTCATAGATCTCC				
TiPV-VP1-F	ATGACCGAATTACTATTAGTAC GTTG	1665	<i>VP</i> , TiPV	Gene amplification	This study
TiPV-VP1-R	CTACGTAGCTGTCCCACCTGA				
TiPV-Fq & TiPV-NS1-R	As above	359	<i>NS1</i> , TiPV	Probe preparation	As above
SagroEL-F	AGCTGTTAAAGCGCCTGGAT	142	<i>groEL</i> , <i>S. agalactiae</i>	qPCR detection	Leigh et al., 2019
SagroEL-R	AGCAGACTGTCCTAAACTTGC				
SagroEL-P	(FAM)-CCAGCATGGCTTACGACGATCA-(BHQ)				
F13N	TGTTTATGCTTGGATGGAA	282	<i>RdRp</i> , IMNV	Probe preparation	Senapin et al., 2007
R13N	TCGAAAGTTGGCTGATG				

328

329 **Table 2:** Summary of diagnostic results

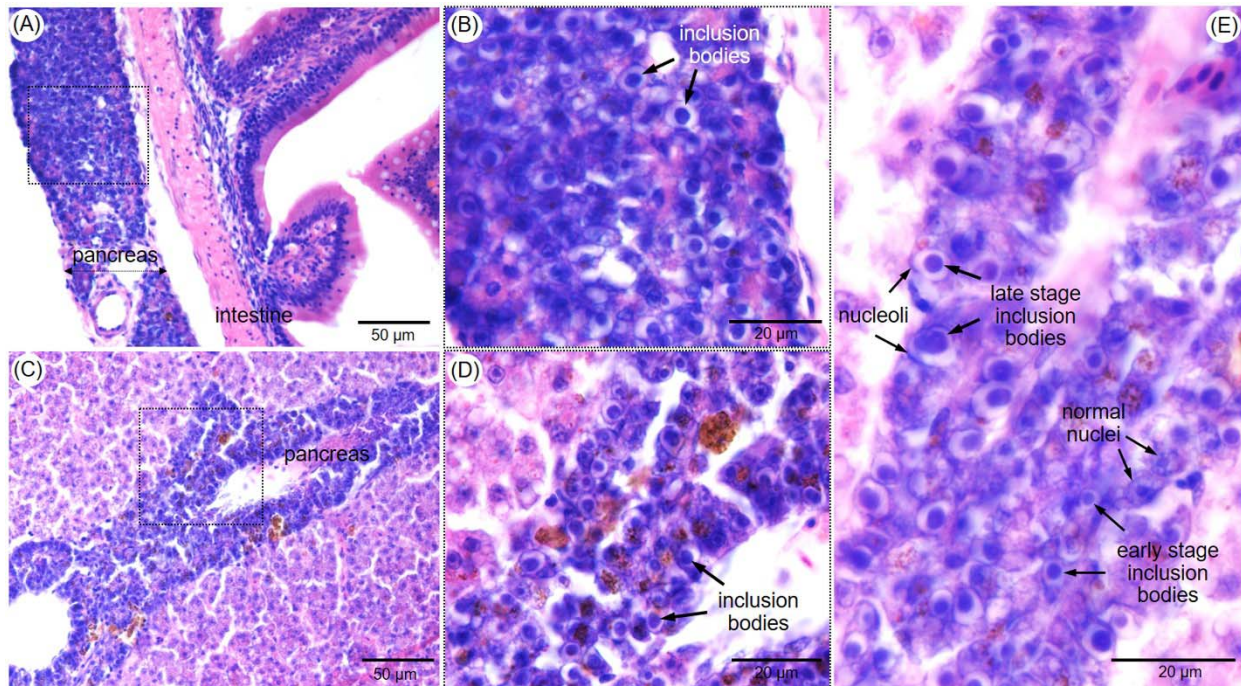
Fish	Histopathology		TiPV qPCR (Cq)	<i>S. agalactiae</i> qPCR (Cq)	Recovery of <i>S. agalactiae</i>
	Cowdry type A inclusion body	Granulomas			
F1	+	+	+ (20.16)	+ (34.86)	-
F2	+	+	+ (18.62)	+ (37.10)	+
F3	+	+	+ (23.14)	+ (33.61)	-
F4	+	+	+ (23.44)	+ (35.49)	+
F5	+	-	+ (20.11)	+ (35.27)	-
F6	+	+	+ (29.87)	+ (34.88)	+
F7	+	+	ND	ND	-
F8	+	-	+ (26.89)	-	-
F9	ND	ND	+ (21.74)	-	-
F10	+	-	+ (25.18)	-	ND

330 +, positive; -, negative; ND, not done



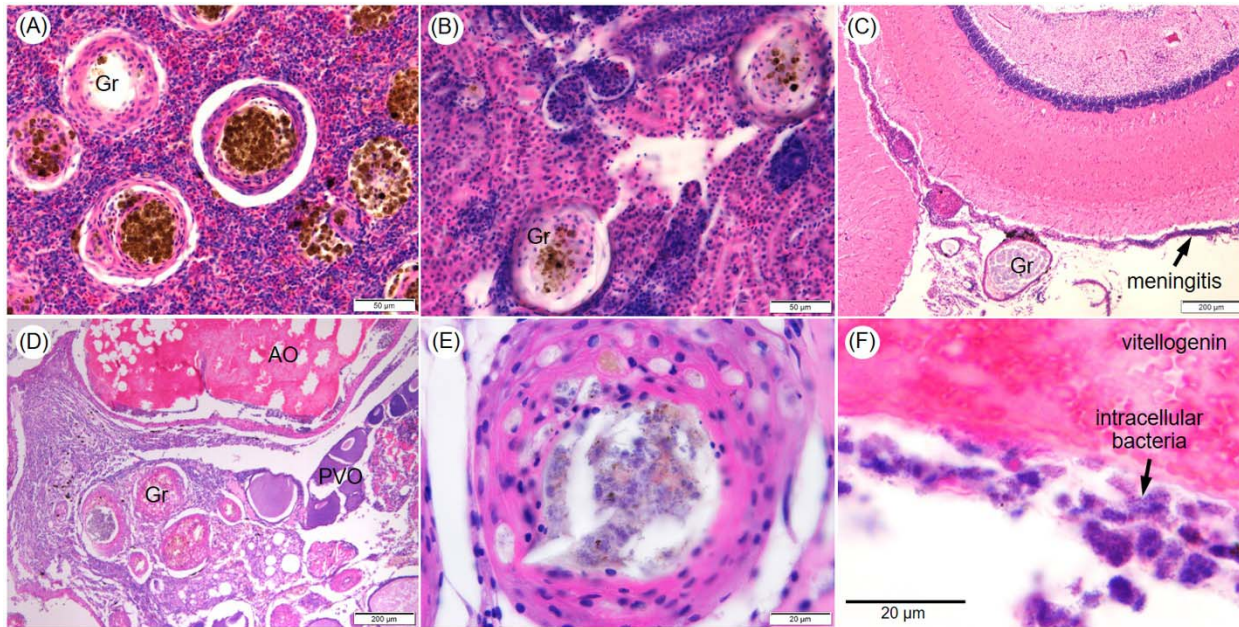
331

332 **Figure 1.** Gross signs of Nile tilapia naturally infected with TiPV showing corneal injury (A),
333 cloudy eye lens (B), liver atrophy, intestinal pallor and necrotic ovary (C).

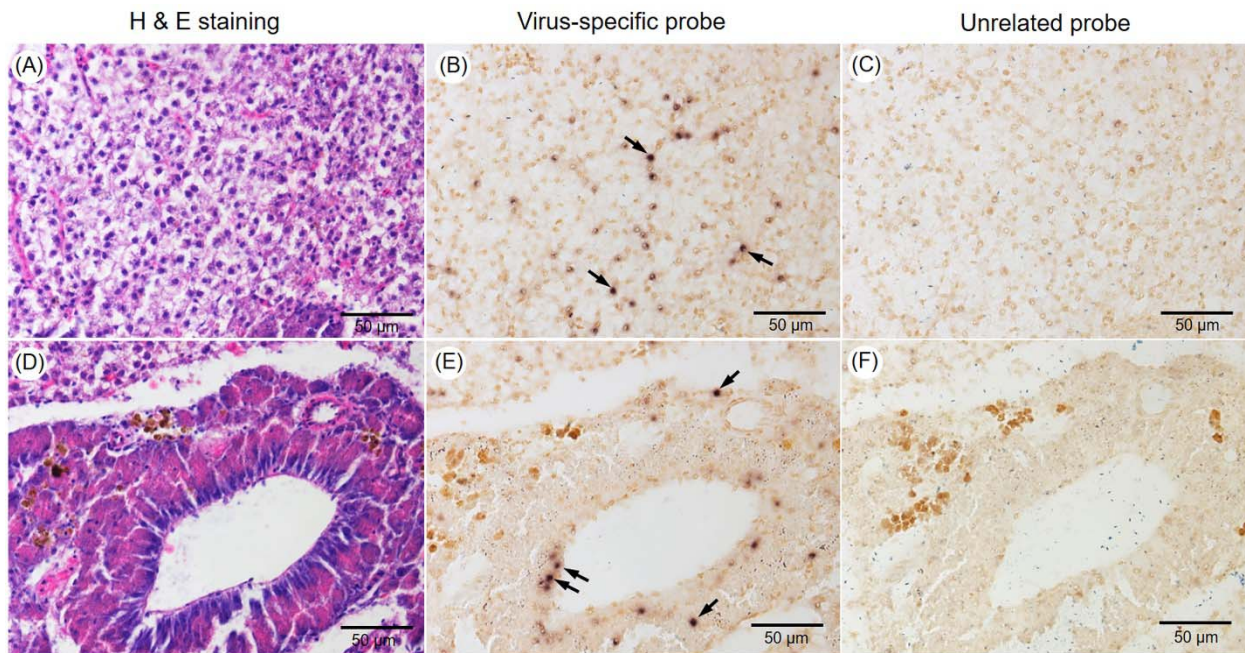


334

335 **Figure 2.** Microphotographs of H&E-stained sections of the pancreatic tissue along the intestine
336 (A-B) and within the hepatopancreas (C-E) of clinically sick tilapia infected with TiPV. Pictures
337 B and D are higher magnification images of the areas marked with dotted boxes in A and C,
338 respectively. Typical Cowdry type A inclusion bodies are visualized in B and D. Early and late-
339 stage inclusion bodies are clearly observed in the pancreatic cells (E).

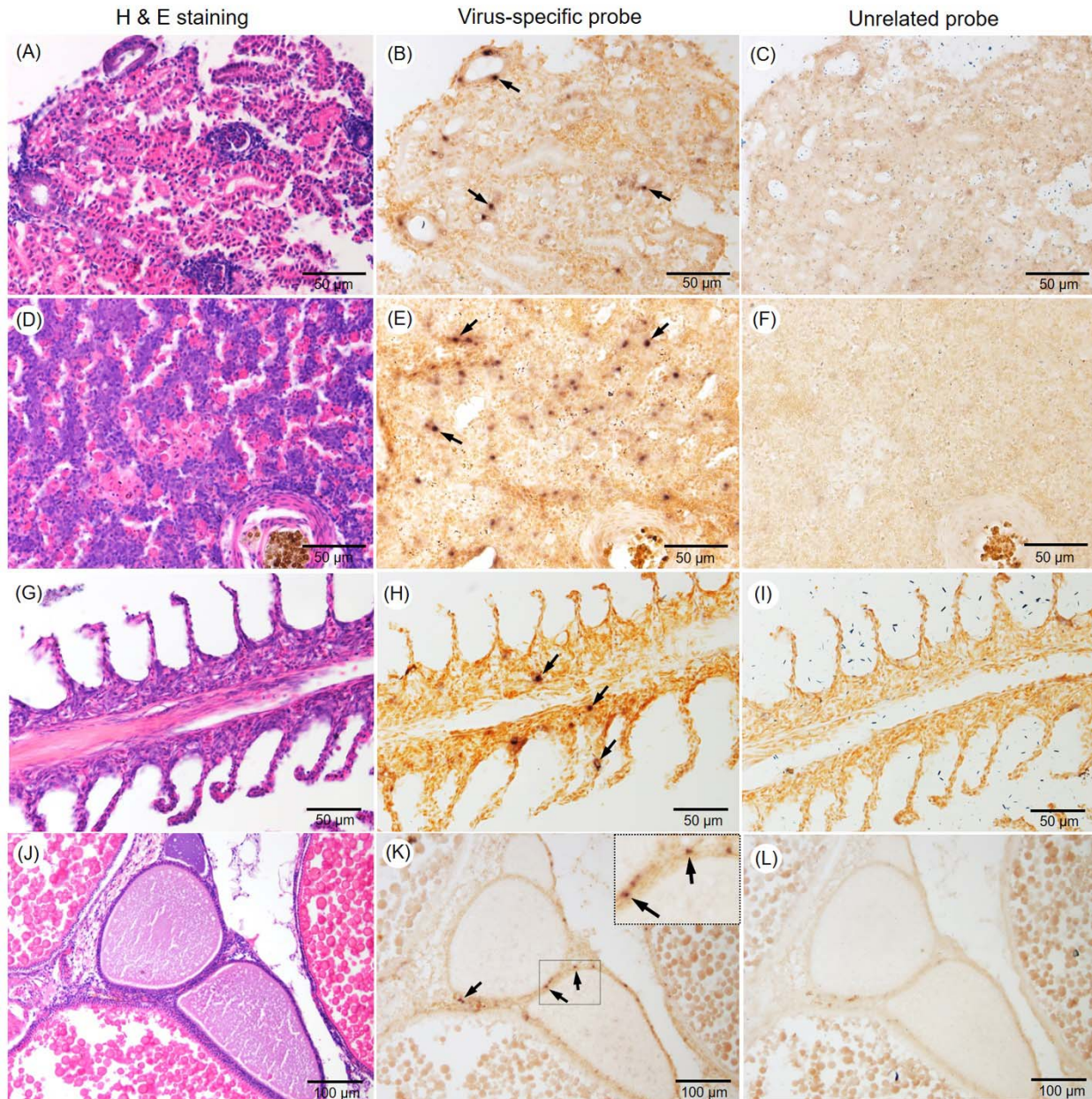


340
341 **Figure 3.** Representative microphotographs of the spleen (A), kidney (B), brain (C) and ovary
342 (D) sections of a clinically sick tilapia showing presence of granulomas containing intralesional
343 pigment (melanin), and increased melanomacrophage centers. Severe meningitis was observed in
344 the brain (arrow, C). High magnification of a typical granuloma showing numerous bacterial
345 coccii in the center (E). Numerous intracellular bacterial coccii on the membrane of oocytes in the
346 ovary (arrow, F). AO, atretic oocyte; PVO, pre-vitellogenic oocytes; Gr, granuloma. H&E
347 staining.



348

349 **Figure 4.** Representative photomicrographs of three continuous sections of the hepatopancreas
350 (A-C) and pancreas (D-F) of a TiPV infected tilapia. H&E-stained sections (A, D), ISH with
351 TiPV-specific probe (B, E), and ISH with unrelated probe (C, F – negative control). A positive
352 signal is characterized by intranuclear dark brown staining, which is multifocal in both
353 hepatocytes and pancreas (arrows in B and E).



354

355 **Figure 5.** Representative photomicrographs of three continuous sections of kidney (A-C), spleen
356 (D-F), gills (G-I), and ovary (J-L) of TiPV infected tilapia. H&E-stained sections (A, D, G and
357 J), ISH with TiPV-specific probe (B, E, H and K), and ISH with unrelated probe (C, F, I and L).
358 TiPV positive signals are indicated by intranuclear dark brown staining (arrows).